



**HAL**  
open science

# Using Artificial Intelligence to identify CMIP6 models from daily SLP maps

Pascal Yiou, Soulivanh Thao

► **To cite this version:**

Pascal Yiou, Soulivanh Thao. Using Artificial Intelligence to identify CMIP6 models from daily SLP maps. 2025. hal-04959475

**HAL Id: hal-04959475**

**<https://hal.science/hal-04959475v1>**

Preprint submitted on 20 Feb 2025

**HAL** is a multi-disciplinary open access archive for the deposit and dissemination of scientific research documents, whether they are published or not. The documents may come from teaching and research institutions in France or abroad, or from public or private research centers.

L'archive ouverte pluridisciplinaire **HAL**, est destinée au dépôt et à la diffusion de documents scientifiques de niveau recherche, publiés ou non, émanant des établissements d'enseignement et de recherche français ou étrangers, des laboratoires publics ou privés.

# Using Artificial Intelligence to identify CMIP6 models from daily SLP maps

Pascal Yiou<sup>1\*</sup> and Soulivanh Thao<sup>1</sup>

<sup>1</sup>Laboratoire des Sciences du Climat et de l'Environnement, UMR 8212 CEA-CNRS-UVSQ, IPSL and U. Paris-Saclay, CE l'Orme des Merisiers, Gif-sur-Yvette, 91191, France.

\*Corresponding author(s). E-mail(s): [pascal.yiou@lsce.ipsl.fr](mailto:pascal.yiou@lsce.ipsl.fr);  
Contributing authors: [soulivanh.thao@lsce.ipsl.fr](mailto:soulivanh.thao@lsce.ipsl.fr);

## Abstract

Large databases of climate model simulations are essential to sample climate variability and estimate how it can evolve in any future. The chaotic nature of climate has motivated the simulation of large ensembles of simulations, which sample the uncertainty due to internal climate variability in single models. Exploiting large ensembles (for impact or attribution studies) implicitly relies on the hypothesis that simulations are interchangeable. This is not the case for variables like temperature, due to biases (which can be corrected). Some synoptic fields, like SLP, do not yield obvious biases, which might justify their use to enrich reanalysis data. In this paper, we examine this hypothesis through a neural network classification approach. The goal is to determine whether it is possible to recognize a climate model (among 16 models and a reanalysis) from one single sea-level pressure (SLP) map over the North Atlantic. We find that models are highly identifiable in the summer (and less in other seasons), while SLP average structures are very similar. From this classification, we identify similarities of climate models, and investigate how climate change can affect SLP daily patterns toward the end of the 21st century. This study allows identifying which climate models could be used as input for artificial intelligence model forecasts.

**Keywords:** Neural Network, classification, Climate models, SLP

001  
002  
003  
004  
005  
006  
007  
008  
009  
010  
011  
012  
013  
014  
015  
016  
017  
018  
019  
020  
021  
022  
023  
024  
025  
026  
027  
028  
029  
030  
031  
032  
033  
034  
035  
036  
037  
038  
039  
040  
041  
042  
043  
044  
045  
046

# 047 1 Introduction

048  
049 Describing and understanding climate variability poses major computational, statis-  
050 tical and physical challenges. Some of the issues are treated by considering ensembles  
051 of coupled global climate model (GCM) simulations, i.e., with several climate mod-  
052 els, and running several simulations. Then averages and other statistical moments  
053 are computed from those large datasets [1]. An other ambition that motivates the  
054 generation and use of those large climate datasets is to consider them as surrogates  
055 of the real world to learn how to forecast the weather [2], or provide extreme event  
056 attribution statements [3]. Those endeavors (computing statistical moments, transfer  
057 learning) make the implicit assumption that all climate models yield similar proba-  
058 bility distributions, and that those statistical properties are the same as observations.  
059 There are many ways of removing model biases, in order to get close to this impor-  
060 tant assumption [4, 5], but those methods are rarely devised for fields (with space and  
061 time).

062 Even if a meteorological field obtained from a GCM does not yield obvious biases,  
063 the question we want to address is whether it is possible recognize a GCM from *one*  
064 daily map, like sea-level pressure (SLP). If one can provide such a detection, then  
065 learning from one GCM is certainly useless for other models. If GCMs cannot be  
066 distinguished, then one has a good case for pooling them in order to enlarge the set of  
067 observed climate variability that is limited to a few decades. One of the motivations  
068 of this paper stems from the idea of transfer learning [6, 7], from ensembles of climate  
069 model simulations, to actual weather predictions. In this perspective, learning from a  
070 daily timescale is crucial, in order to investigate extreme events [8].

071 In this paper, we consider the whole CMIP6 archive [9], which contains 47 models  
072 that provide data with daily time steps (Figure A1). We consider daily SLP over the  
073 North Atlantic, between 1970 and 2000. We determine whether it is possible to rec-  
074 ognize a model name from *one* daily SLP map (over the North Atlantic). We use a  
075 simple artificial intelligence (AI) algorithm of classification (a Multi-Layer-Perceptron  
076 neural network [10]) without any particular tuning to learn how to recognize a model  
077 from SLP features, for each season (summer, autumn, winter and spring). The clas-  
078 sification is done along with the ERA5 reanalysis [11]. Hence, this study extends the  
079 garment identification AI challenge [12] to a more sophisticated setting. The analysis  
080 protocol is described in the methods section.

081 If an AI algorithm cannot tell models apart (from daily SLP fields) or from reanal-  
082 yses, then pooling model SLP can be considered a promising in order to enlarge sample  
083 size, in order to build statistical confidence. If an AI algorithm *can* tell models apart,  
084 even though their sample means and standard deviations are similar, then it is not  
085 possible to learn, even from a large simulation ensemble of one model, to infer anything  
086 on the real world.

087 We evaluate whether GCMs can be identified from simulations that are provided in  
088 a different setting from the learning set (different ocean model, different atmospheric  
089 parameterizations, etc.). This study revisits the analyses of [13, 14] by focusing on  
090 daily time scales, which adds a major difficulty to the classification problem, due to  
091 meteorological variability.

092

We determine whether a warmer climate according to SSP scenarios [15] affects the weather patterns of climate models. This is done with the SSP5-8.5 scenario for end-of-the century (2070–2100) period. The Methods section explains the analysis protocols.

## 2 Results

### 2.1 SLP Classification of 16 models

Each daily SLP map was classified onto 16 GCMs and the ERA5 [11] reanalysis (see Methods section, Table A1). The classification was done for the four seasons (Summer: June-July-August (JJA); Fall: September-October-November (SON); Winter: December-January-February (DJF); Spring: March-April-May (MAM)), due to the seasonality of the atmospheric circulation [16].

The training set used  $\approx 22$  years for each model, and the validation set used the remaining  $\approx 8$  years. The training was repeated 20 times, so that 20 AI models are obtained. We report the resulting scores on the validation periods in Figure 1. This reflects the variability of classification scores due to the algorithm itself. In the sequel, we will keep the AI models that yield the best overall scores.

The summer (June-July-August) classification of 16 models and ERA5 reanalysis shows that the AI algorithm can recognize seven models with a success probability larger than 0.6 (Figure 1a). It is possible to enhance the classification score by repeating the neural network training with random samples of 9 GCMs rather than 16. This guarantees that the classification scores exceed 80% for daily SLP (not shown). This procedure is not discussed here, as this study is based on the minimal achievable result with AI and avoiding technical tuning procedures.

For the other seasons (spring, autumn and winter) the AI algorithm classification scores are lower, and rarely pass the 0.6 value (Figure 1b–d). This means that the SLP from 17 models (including ERA5) are difficult to distinguish from one model to another. For DJF, four GCMs can be classified with probabilities larger than 0.6, although the ERA5 reanalysis is poorly classified. For intermediate seasons, three models (for SON) or two models (for MAM) can be classified by probabilities exceeding 0.6. The SLP from the NorCPM1 model is consistently well classified across all seasons. Conversely, the EC-Earth3 model yields consistent low classification probability rates across seasons. The ERA5 reanalysis does not stand out as "recognizable" among the CMIP6 models.

A test procedure with a distinct run for each model and the best AI model in Figure 1 is performed. Figure 2 shows the classification probability distributions onto the 16 CMIP6 models (Table A1) and ERA5, with different historical runs (the test sets). The diagonals indicate whether AI model clearly identifies models from daily SLP fields. We note that, with the best AI model (from Figure 1), the JJA true positive rates exceed  $p = 0.6$ , which means that it is possible to identify a GCM from a daily SLP map, more than 60% of the time, which is better than tossing a coin (and higher than  $p_0 = 1/17$  if all models/ERA5 are equiprobable). We verified that summer SLP can be recognized, for any run of the training models (not shown) with probabilities exceeding 0.6. This means that internal variability does not alter the SLP

139 identification process. We also verified that no obvious bias among GCMs explained  
140 such a classifiability by comparing mean SLP and standard deviations (SI Figure 2).  
141 The spatial structures of SLP (and its variability) are very similar between GCMs, and  
142 naked eyes would have difficulties identifying a model from a single daily SLP map.

143 Those classification probabilities drop during intermediate seasons (SON and  
144 MAM), although models are can still be identified, albeit with scores lower than  
145  $p = 0.3$ . GCMs (or ERA5) cannot be identified from winter (DJF) daily SLP maps  
146 (Figure 2c). The ERA5 reanalysis is not more identifiable than the GCMs. There-  
147 fore, North Atlantic SLP maps of GCMs can hardly be distinguished from reanalyses,  
148 especially in the winter.

149 For all seasons, the EC-Earth model is often confused with the ERA5 reanalysis  
150 (Figure 2), which is explained by the fact that they are based on the same atmospheric  
151 model [17].

152

## 153 2.2 Identification of GCM sororities

154

155 Starting from a classification of 16 models in Table A1, we classify the "sister" models  
156 identified in Figure A1 (black bars). Those GCMs are produced by the same research  
157 groups, but can yield different horizontal resolutions (shown in Supplementary Table  
158 1), or contain different physical configurations [1]. The goal is to check whether the  
159 classification performed on the reference models work for "sister" models, especially  
160 for the summer season.

161 With a couple of exceptions, sororities can be identified with SLP classifica-  
162 tion (Figure 3). When GCMs from different research institutes (e.g. UKESM1 and  
163 HadGEM3 models) share the same atmospheric model (e.g., MOHC) and yield similar  
164 horizontal resolutions, then they tend to be classified to HadGem3-GC31-LL, espe-  
165 cially in JJA. Classifiability does not increase during other seasons. Similarly, models  
166 of the EC-Earth consortium (EC-Earth3-Veg and EC-Earth3-Veg-LR) simulations are  
167 classified to the EC-Earth3 model. The CNRM-ESM2-1 and reference CNRS-ESM1  
168 GCMs differ from their atmospheric chemistry models. This difference does not affect  
169 their SLP sorority in the summer. The NorESM2-LM and NorCPM1 GCMs essentially  
170 differ from their vertical resolution, but their sorority can be identified.

171 The horizontal resolution of MPI-ESM1-2-HR is almost twice the resolution of  
172 MPI-ESM1-2-LR (all submodels are the same, though). This explains that those  
173 two GCMs cannot be classified onto one another in the summer, because the high-  
174 resolution model (which has a fairly high resemblance to ERA5) can yield SLP patterns  
175 that are not obtained with the low reference GCM. Similarly, the FGOALS-I3 model  
176 is nearly twice the resolution of FGOALS-g3, with a different atmospheric code. This  
177 also explains why the summer SLP of the two models (from the same institution) do  
178 not seem similar.

179 Therefore, the daily SLP maps in the summer season (JJA) allow identifying GCM  
180 sororities (Figure 3a) when horizontal resolutions are comparable, while this is much  
181 less clear for other seasons. This implies that the atmospheric circulation from models  
182 of the same family can be "pooled" in order to increase ensemble sizes. This feature  
183 is linked to the intrinsic resolution of the atmospheric model, because all models and  
184 ERA5 were re-interpolated on a  $1^\circ \times 1^\circ$  degree grid.

### 2.3 Influence of climate change

We investigate the SLP classification from the 16 models in Table A1 toward the end of the 21st century in scenario simulations [9, 15]. The scenario we consider here is SSP5-8.5, and we extract the SLP from 2070 to 2100.

The probabilities along the diagonal in JJA (Figure 4a) slightly decrease in the summer, implying a slight increase of "misclassification". This suggests that some models witness the appearance of new SLP patterns (with respect to their own 1970–2000 behavior) towards the end of the 21st century, and that those patterns were sampled in other GCMs.

The highest classification rates for intermediate seasons (SON and MAM) still appear on the diagonals of Figure 4bd (the NorCPM1 model does not propose daily SLP for SSP simulations and hence does not appear). This identification no longer holds for winter SLP (Figure 4c). The overall similarity between Figures 2 and 4 suggests that the SLP patterns of climate models are barely affected by climate change, even in an extreme SSP5-8.5 scenario. Other SSPs show a similar behavior (not shown).

There is one exception to this stability: the NESM3 model whose SSP5-8.5 winter classification never finds SLP patterns in historical simulations of the same model in 1970-2000 (upper right corner in Figure 4). This means that this model yields a change in winter atmospheric circulation.

## 3 Discussion

The classification results of this study are based on a fairly simple use of a neural network, without any particular tuning (e.g. low number of layers of neurons, simple algorithm, no convolutional layer, etc.). For example, only one hidden layer of 256 neurons is sufficient to correctly classify summer SLP. The training sets (2000 days for each model) are small, compared to what is potentially available in the CMIP6 archive. This choice is made to avoid overfitting. The classification scores could be improved by considering larger training sets or tuning neural network parameters, although the dependence on the season would remain unchanged.

Using other climate fields (temperature, precipitation, wind speed) would be possible, but since they highly depend on the model horizontal resolution and other idiosyncrasies like local biases, it is expected that model classifiability could be enhanced in a fairly trivial way. Hence, this type of analysis would be interesting to test the effects of multi-variate bias correction on a CMIP6 ensemble and reanalysis data. [18] used this strategy to design bias correction models, where a bias-correction model is trained so that a classifier is not able to recognize a bias corrected field from a reanalysis field.

It has been argued that internal climate variability is a major source of uncertainty for climate assessments [19, 20], as members of ensemble simulations could show different behavior. Such studies hence suggest that simulations of the same climate model should be treated separately, as their variability might differ. Our study brings a nuance by showing that simulation ensembles of the same model do yield an identifiable consistency, while the role of internal variability is more important in the winter season, which leads to a lack of classification skill.

185  
186  
187  
188  
189  
190  
191  
192  
193  
194  
195  
196  
197  
198  
199  
200  
201  
202  
203  
204  
205  
206  
207  
208  
209  
210  
211  
212  
213  
214  
215  
216  
217  
218  
219  
220  
221  
222  
223  
224  
225  
226  
227  
228  
229  
230

## 231 4 Conclusion

232 We outlined the intriguing faculty of identifying a climate model from one daily SLP  
233 map, with a simple neural network. This property is essentially valid for the summer  
234 season. The 16 reference training models we considered are not only different from  
235 each other, but they are also different from the ERA5 reanalysis on the present-day  
236 period. It is much more difficult to differentiate the SLP from models and reanalysis  
237 for other seasons, which is also an interesting feature, because one can pool models in  
238 order to increase the sampling of data in a meaningful way.

239 This rather simple approach also allows us to identify the sorority of climate mod-  
240 els. This means that different flavors of the same model (increasing resolution, changing  
241 land-use schemes, or even changing the ocean model) lead to similar atmospheric prop-  
242 erties in the midlatitude regions (at least the North Atlantic), and hence shows the  
243 robustness of the atmospheric part of coupled models, especially in the summer.  
244

245 AI-based weather forecast systems have been trained on the ERA5 reanalysis [8,  
246 21]. It is tempting to use a larger data base for training in order to have a better  
247 sampling of interannual atmospheric variability [7]. This study shows that it would  
248 be misleading to take any climate model, because of the different spatial probability  
249 distributions of atmospheric variables between models, and it would require complex  
250 bias correction. This study has outlined good candidate GCMs (with large ensembles,  
251 similarities with ERA5) for this exercise.

252 Conversely, this also implies that the statistical properties of the atmospheric cir-  
253 culation from large ensemble model simulations (with the same model [22]) can be  
254 enriched with variations around the same model, provided that the horizontal resolu-  
255 tions are similar. Therefore, it makes sense to "pool" climate model simulations of the  
256 same family, to perform extreme event attribution analyses.

257

## 258 5 Data and Methods

259

### 260 5.1 Data

261 This study focuses on North Atlantic [50W–20E; 30N–65N] daily SLP fields from the  
262 CMIP6 [9] archive. The SLP fields were extracted for all runs of global climate models  
263 (GCMs) that propose daily fields for historical and SSP simulations [15]. We restricted  
264 the analysis to the data that is available on the IPSL database server, which is a subset  
265 of the ESGF data <https://esgf-node.ipsl.upmc.fr/projects/esgf-ipsl/>. For simplicity,  
266 some models (e.g. with only one member) were not used in this study (black lines in  
267 Figure A1).

268 We focus on the North Atlantic region (SI Figure 1), although other regions of  
269 the world could have been used, because this is where climate models seem to yield a  
270 large consensus [23]. SLP patterns marginally depend on climate change (unlike many  
271 other climate fields) [24], although the patterns yield a seasonal cycle [16]. Hence  
272 investigating North Atlantic SLP classification is deemed a difficult endeavor.

273 For training, we chose 16 GCMs (out of 47) because they yield the largest number  
274 of runs (and more than 3), and reflect the diversity of atmospheric models, as climate  
275

276

modeling groups can provide simulations with variations on the resolution, ocean model, etc. [1].

In the training set, we considered the first 2000 days (for each season) in historical simulations, from 1970 to 2000, which corresponds to  $\approx 22$  years (hence 1970 to 1992). We used the first simulations in lexicographic order for the training set. For validation, we used the remaining  $\approx 8$  years of the same simulation. The test set included historical simulations (1970–2000) from the third simulations in lexicographic order (this choice was arbitrary). Therefore, the test sets (in Figures 2 to 4) are disjoint from the learning set.

For all models, the SLP fields were normalized by their average. Therefore, models cannot be identified by a potential bias in the mean, which is difficult to identify. The spatial standard deviations are rather similar across models (SI Figure 2).

All SLP fields (CMIP6 and ERA5) are interpolated onto  $1^\circ \times 1^\circ$  degree maps. Therefore information on the horizontal resolution of each model is not used in the classification.

The tests sets include other runs from the same model, runs from other models (black lines in Figure A1), and scenario runs until the end of the 21st century. In this paper, we focused on the SSP5-8.5 (although computations were done for all SSPs [25]). This scenario might not be the most relevant for society [26], but it allows a higher signal-to-noise ratio, to identify responses of climate change.

## 5.2 Methods

The AI classification model we use is a basic method of image classification [10, 27], that can be used to identify clothes from pictures [12].

The AI model is a simple dense neural network with a single hidden layer of 256 neurons with relu activation functions and an output layer of 17 neurons (the maximum number of GCMs) with a softmax activation functions. The dense neural network use as inputs SLP fields flattened into vectors of  $70 \times 36 = 2520$  values.

The neural network model (AI model) is trained over the training set constructed from models listed in Table A1. 5 epochs are used in the training and sparse categorical cross-entropy is optimized, with an adam optimizer. The training is repeated 20 times, because this procedure yields random selections of input data and weight initialization. At each new training step, we compute the score rate, i.e., the probability of correctly classifying an SLP field on a validation set, which is different from the training set. The scores of this procedure are shown in Figure 1, for validation sets that consist of other historical simulations. For each season, we keep the AI model that yields the highest score.

Those AI models are used to classify models that are *not* listed in Table A1. This helps identifying potential "sororities", when GCMs share common atmospheric components.

Then the AI models (for historical periods) are used to classify scenario simulations (SSP5-8.5) to track potential drifts in daily SLP patterns.

In Figure 1 we consider an arbitrary score probability of  $p = 0.6 > 0.5$ , which is higher than a "coin toss" probability and much higher than an equiprobable classification value over the 17 models of  $p = 1/17 \approx 0.06$ .



## 323 6 Figures

324

325

326

327

328

329

330

331

332

333

334

335

336

337

338

339

340

341

342

343

344

345

346

347

348

349

350

351

352

353

354

355

356

357

358

359

360

361

362

363

364

365

366

367

368

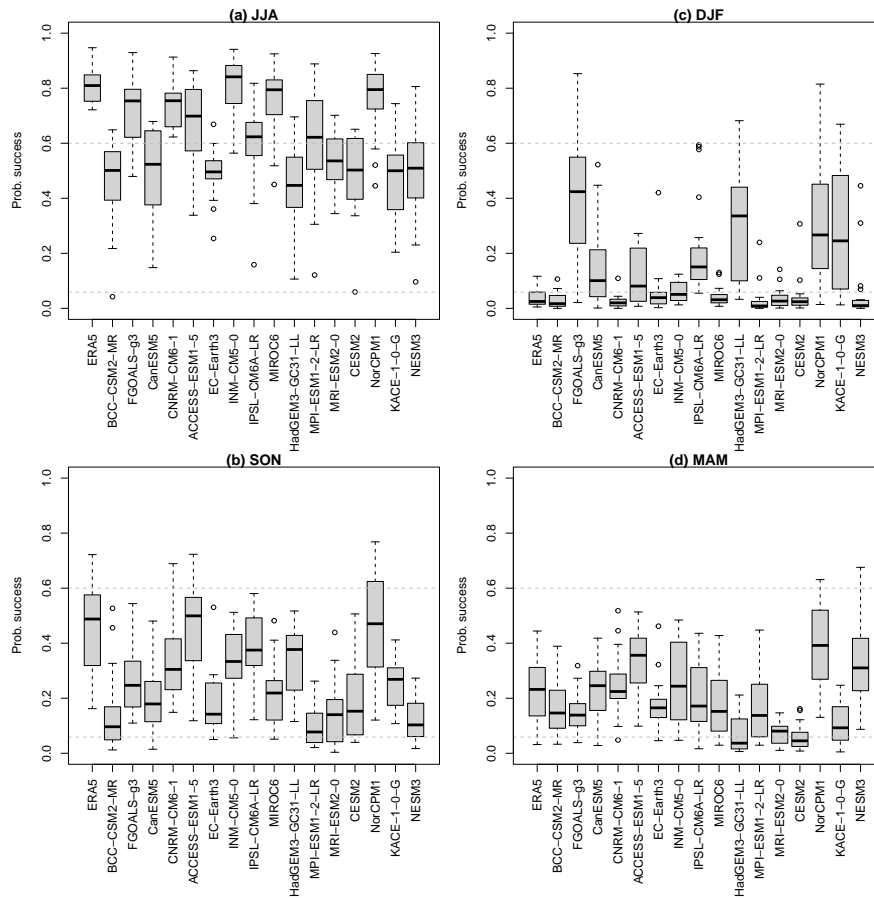


**Fig. 1** Empirical probabilities that 16 CMIP6 models or ERA5 are correctly classified for each season (panels a to d). 20 training classifications were performed. The boxplots reflect the variability of the score probabilities of the training procedure (20 classifications). The horizontal dashed line represents the threshold probabilities  $p = 0.6$  and  $p = 1/17$  (a uniformly random classification).

**Supplementary information.** This article comes with supplementary information, with a table of all CMIP6 models that are considered, and summary figures.

**Acknowledgements.** Some ideas of this study emerged from discussions with colleagues at Météo-France (Enora Cariou, Julien Cattiaux and Aurélien Ribes). We thank the IPSL ESPRI group for maintaining the CMIP6 archive. Most computations were done with the IPSL GPU server.

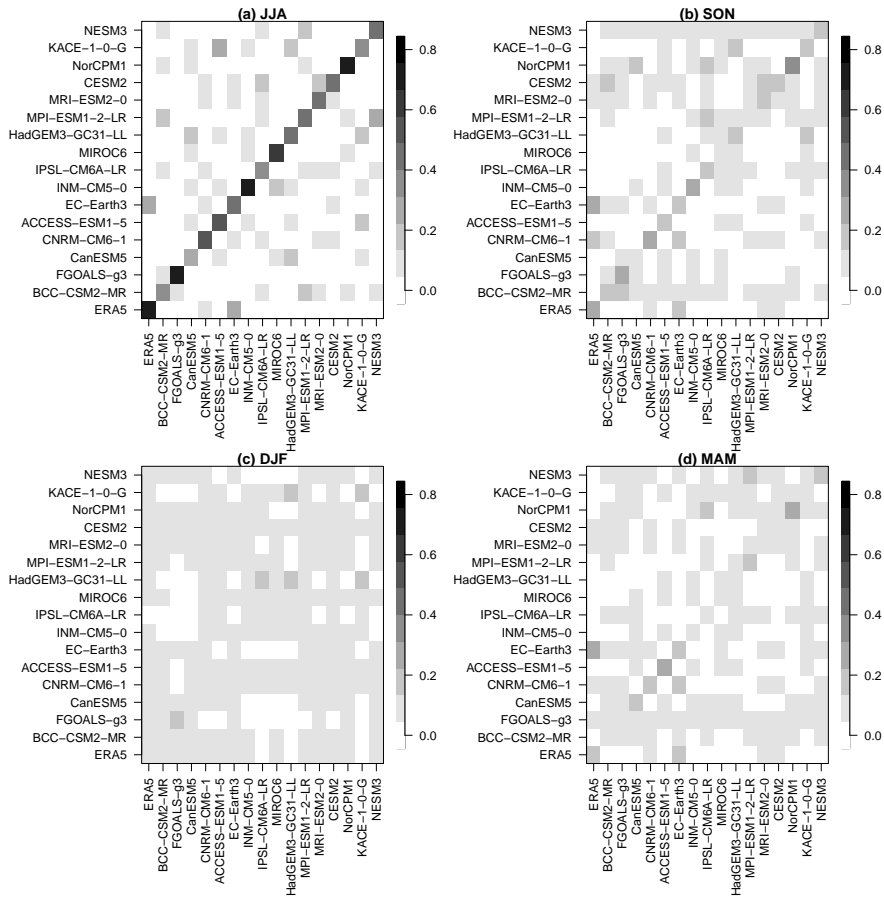


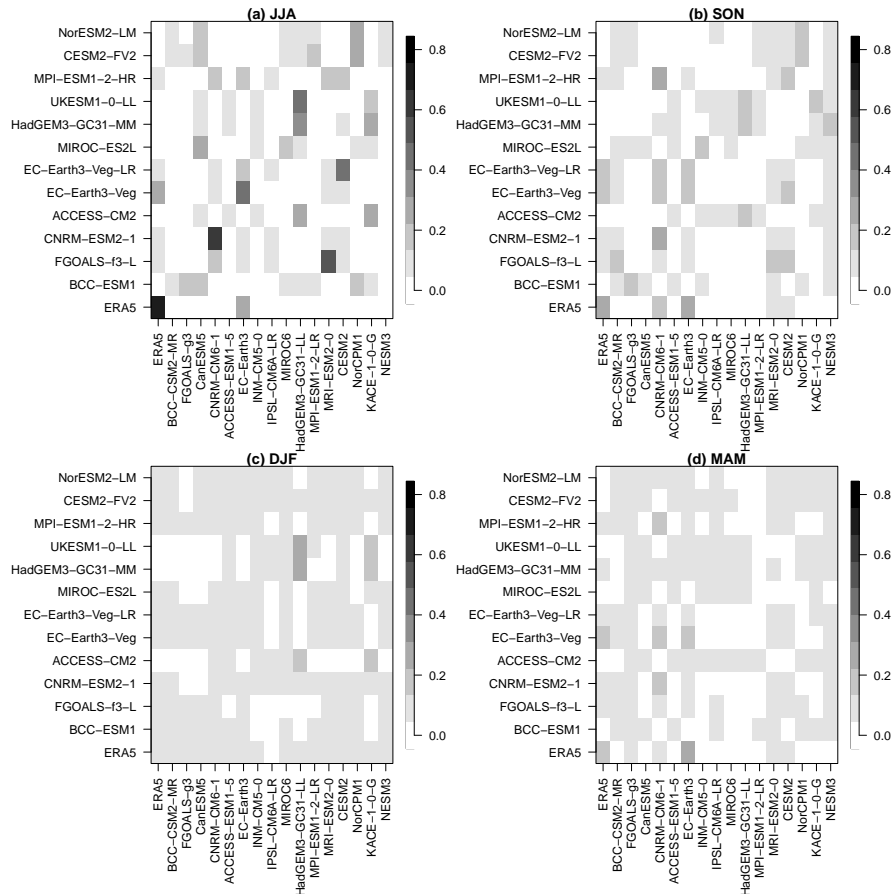
**Fig. 2** Classification test. Empirical probabilities of classifying CMIP6 models in Table A1 or ERA5 onto those models, for the four seasons (panels a to d). Darker colors indicate higher probabilities. In those diagrams, the sum of probabilities along lines is 1. Model simulations listed on the vertical axis are classified onto the list of models on the horizontal axis. In this figure, the two lists of names coincide.

## Declarations

- Funding: This work received the support of the grant ANR-20-CE01-0008-01 (SAM-PRACE) and from Agence Nationale de la Recherche - France 2030, as part of the PEPR TRACCS programme under ANR-22-EXTR-0002. This work also received support from the European Union's Horizon 2020 research and innovation programme under grant agreement No. 101003469 (XAIDA).
- The author declare no competing interests.
- Data availability: ERA5 data was extracted from the climate explorer (<https://climexp.knmi.nl/>). CMIP6 data is available on ESGF nodes (e.g. <https://esgf-node.ipsl.upmc.fr/projects/esgf-ipsl/>). We used the data that is available on the IPSL data server.

369  
370  
371  
372  
373  
374  
375  
376  
377  
378  
379  
380  
381  
382  
383  
384  
385  
386  
387  
388  
389  
390  
391  
392  
393  
394  
395  
396  
397  
398  
399  
400  
401  
402  
403  
404  
405  
406  
407  
408  
409  
410  
411  
412  
413  
414

415  
416  
417  
418  
419  
420  
421  
422  
423  
424  
425  
426  
427  
428  
429  
430  
431  
432  
433  
434  
435  
436  
437  
438  
439  
440  
441  
442



443 **Fig. 3** Sorority classification. Empirical probabilities of classifying CMIP6 models (blue lines in Fig.  
444 A1 onto CMIP6 models in Table A1 or ERA5, for the four seasons (panels a to d). Darker colors  
445 indicate higher probabilities. Model simulations listed on the vertical axis are classified onto the list  
446 of models on the horizontal axis.

- 447 • Code availability: the codes for preparing CMIP6 files, and classification are  
448 available on from <https://github.com/pascalyiou/CMIP6-CNN-Classification.git>.
- 449 • Author contribution: PY conceived and performed the analyses, and wrote the  
450 manuscript. ST advised on the neural network implementation and contributed to  
451 the writing of the manuscript.

## 454 References

456 [1] Intergovernmental Panel On Climate Change (Ippc). in *Annex II: Models 1*  
457 edn, (ed.Gutiérrez, J M., A.-M. Tréguier) *Climate Change 2021 – The Physical*  
458 *Science Basis: Working Group I Contribution to the Sixth Assessment Report*  
459 *of the Intergovernmental Panel on Climate Change*. 2087–2138 (Cambridge Uni-  
460 versity Press, 2023). URL <https://www.cambridge.org/core/product/identifier/>

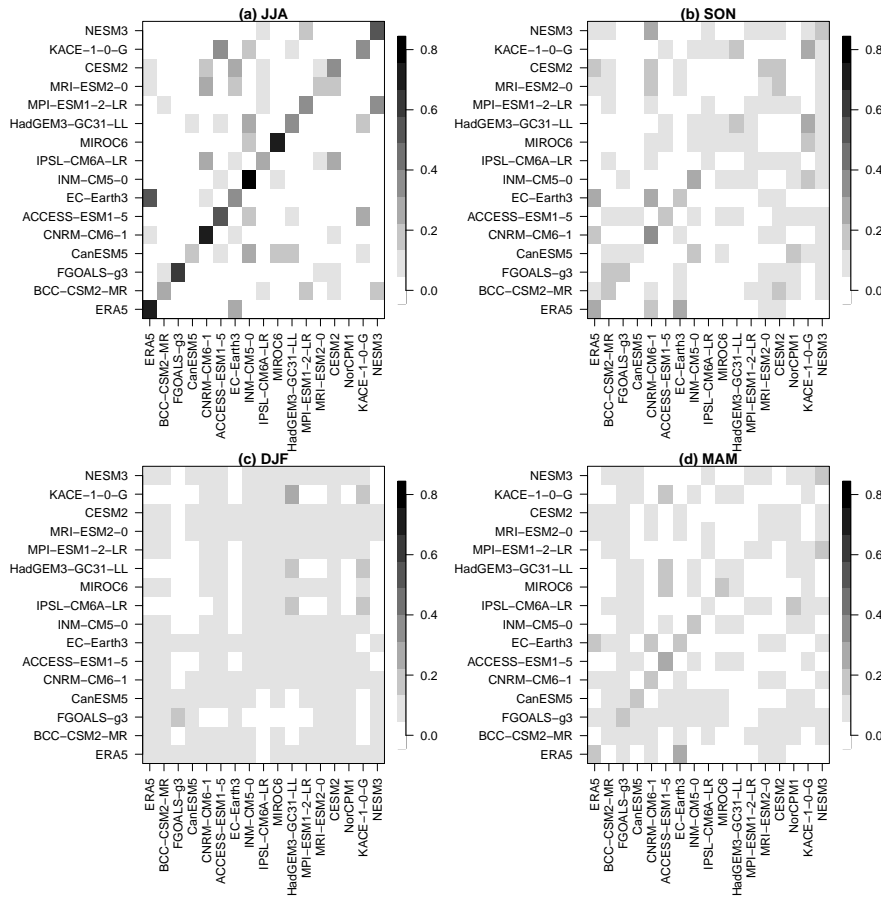


**Fig. 4** Climate change classification. Empirical probabilities of classifying CMIP6 models in Table A1 or ERA5 for SSP5-8.5 simulations (2070–2100) onto those models (historical period: 1970–2000), for the four seasons (panels a to d). Darker colors indicate higher probabilities. Model SSP5-8.5 simulations listed on the vertical axis are classified onto historical simulations listed on the horizontal axis.

[9781109157896/type/book](https://doi.org/10.1002/9781109157896/type/book).

- [2] Kochkov, D. *et al.* Neural general circulation models for weather and climate. *Nature* **632**, 1060–1066 (2024). ISBN: 0028-0836 Publisher: Nature Publishing Group UK London.
- [3] National Academies of Sciences Engineering and Medicine (ed.) *Attribution of Extreme Weather Events in the Context of Climate Change* (The National Academies Press, Washington, DC, 2016). URL [www.nap.edu/catalog/21852/attribution-of-extreme-weather-events-in-the-context-of-climate-change](http://www.nap.edu/catalog/21852/attribution-of-extreme-weather-events-in-the-context-of-climate-change).
- [4] Vrac, M. Multivariate bias adjustment of high-dimensional climate simulations: the Rank Resampling for Distributions and Dependences (R 2 D 2) bias

461  
462  
463  
464  
465  
466  
467  
468  
469  
470  
471  
472  
473  
474  
475  
476  
477  
478  
479  
480  
481  
482  
483  
484  
485  
486  
487  
488  
489  
490  
491  
492  
493  
494  
495  
496  
497  
498  
499  
500  
501  
502  
503  
504  
505  
506

- 507 correction. *Hydrology and Earth System Sciences* **22**, 3175 (2018).  
508
- 509 [5] Robin, Y., Vrac, M., Naveau, P. & Yiou, P. Multivariate stochastic bias  
510 corrections with optimal transport. *Hydrology and Earth System Sciences Discus-*  
511 *sions* **2018**, 1–25 (2018). URL [https://www.hydrol-earth-syst-sci-discuss.net/](https://www.hydrol-earth-syst-sci-discuss.net/hess-2018-281/)  
512 [hess-2018-281/](https://www.hydrol-earth-syst-sci-discuss.net/hess-2018-281/).
- 513 [6] Anwar, H. *et al.* Intercomparison of deep learning models in predicting streamflow  
514 patterns: insight from CMIP6. *Scientific Reports* **14**, 17468 (2024). URL [https://](https://www.nature.com/articles/s41598-024-63989-7)  
515 [www.nature.com/articles/s41598-024-63989-7](https://www.nature.com/articles/s41598-024-63989-7).
- 516 [7] Huang, B., Liu, Z., Duan, Q., Rajib, A. & Yin, J. Unsupervised deep learning bias  
517 correction of CMIP6 global ensemble precipitation predictions with cycle gener-  
518 ative adversarial network. *Environmental Research Letters* **19**, 094003 (2024).  
519 URL <https://iopscience.iop.org/article/10.1088/1748-9326/ad66e6>.
- 520 [8] Lam, R. *et al.* Learning skillful medium-range global weather forecasting. *Science*  
521 **382**, 1416–1421 (2023). URL <https://doi.org/10.1126/science.adi2336>. Publisher:  
522 American Association for the Advancement of Science.
- 523 [9] Eyring, V. *et al.* Overview of the Coupled Model Intercomparison Project Phase 6  
524 (CMIP6) experimental design and organization. *Geoscientific Model Development*  
525 **9**, 1937–1958 (2016).
- 526 [10] Murphy, K. P. *Probabilistic machine learning: an introduction* Adaptive compu-  
527 tation and machine learning (The MIT Press, Cambridge, Massachusetts London,  
528 England, 2022).
- 529 [11] Hersbach, H. *et al.* The ERA5 global reanalysis. *Quat. J. Roy. Met. Soc.* **146**,  
530 1999–2049 (2020). ISBN: 0035-9009 Publisher: Wiley Online Library.
- 531 [12] Leithardt, V. Classifying garments from fashion-MNIST dataset through CNNs.  
532 *Advances in Science, Technology and Engineering Systems Journal* **6**, 989–994  
533 (2021).
- 534 [13] Masson, D. & Knutti, R. Climate model genealogy: climate model genealogy.  
535 *Geophysical Research Letters* **38**, L08703 (2011). URL [http://doi.wiley.com/10.](http://doi.wiley.com/10.1029/2011GL046864)  
536 [1029/2011GL046864](http://doi.wiley.com/10.1029/2011GL046864).
- 537 [14] Knutti, R., Masson, D. & Gettelman, A. Climate model genealogy: Generation  
538 CMIP5 and how we got there. *Geophysical Research Letters* **40**, 1194–1199 (2013).  
539 URL <https://agupubs.onlinelibrary.wiley.com/doi/10.1002/grl.50256>.
- 540 [15] Riahi, K. *et al.* The Shared Socioeconomic Pathways and their energy, land use,  
541 and greenhouse gas emissions implications: An overview. *Global environmental*  
542 *change* **42**, 153–168 (2017). ISBN: 0959-3780 Publisher: Elsevier.
- 543  
544  
545  
546  
547  
548  
549  
550  
551  
552

- [16] Vrac, M., Vaittinada Ayar, P. & Yiou, P. Trends and variability of seasonal weather regimes. *International Journal of Climatology* **34**, 472–480 (2014). URL <https://rmets.onlinelibrary.wiley.com/doi/10.1002/joc.3700>. 553  
554  
555
- [17] Döscher, R. *et al.* The EC-Earth3 Earth system model for the Coupled Model Intercomparison Project 6. *Geoscientific Model Development* **15**, 2973–3020 (2022). URL <https://gmd.copernicus.org/articles/15/2973/2022/>. 556  
557  
558  
559
- [18] François, B., Thao, S. & Vrac, M. Adjusting spatial dependence of climate model outputs with cycle-consistent adversarial networks. *Climate Dynamics* **57**, 3323–3353 (2021). URL <https://link.springer.com/10.1007/s00382-021-05869-8>. 560  
561  
562  
563
- [19] Hawkins, E. & Sutton, R. The Potential to Narrow Uncertainty in Regional Climate Predictions. *Bulletin of the American Meteorological Society* **90**, 1095–1108 (2009). URL <https://journals.ametsoc.org/doi/10.1175/2009BAMS2607.1>. 564  
565  
566  
567
- [20] Deser, C., Terray, L. & Phillips, A. S. Forced and internal components of winter air temperature trends over North America during the past 50 years: Mechanisms and implications. *Journal of Climate* **29**, 2237–2258 (2016). ISBN: 0894-8755 Publisher: American Meteorological Society. 568  
569  
570  
571  
572
- [21] Price, I. *et al.* Probabilistic weather forecasting with machine learning. *Nature* (2024). URL <https://www.nature.com/articles/s41586-024-08252-9>. 573  
574  
575
- [22] Bevacqua, E. *et al.* Advancing research on compound weather and climate events via large ensemble model simulations. *Nature Communications* **14**, 2145 (2023). ISBN: 2041-1723 Publisher: Nature Publishing Group UK London. 576  
577  
578  
579
- [23] Fernandez-Granja, J. A., Casanueva, A., Bedia, J. & Fernandez, J. Improved atmospheric circulation over Europe by the new generation of CMIP6 earth system models. *Climate Dynamics* **56**, 3527–3540 (2021). URL <https://link.springer.com/10.1007/s00382-021-05652-9>. 580  
581  
582  
583
- [24] Cusinato, E., Rubino, A. & Zanchettin, D. Winter Euro-Atlantic Climate Modes: Future Scenarios From a CMIP6 Multi-Model Ensemble. *Geophysical Research Letters* **48**, e2021GL094532 (2021). URL <https://agupubs.onlinelibrary.wiley.com/doi/10.1029/2021GL094532>. 584  
585  
586  
587  
588
- [25] Meinshausen, M. *et al.* The shared socio-economic pathway (SSP) greenhouse gas concentrations and their extensions to 2500. *Geoscientific Model Development* **13**, 3571–3605 (2020). URL <https://gmd.copernicus.org/articles/13/3571/2020/>. 589  
590  
591  
592
- [26] Meinshausen, M. *et al.* A perspective on the next generation of Earth system model scenarios: towards representative emission pathways (REPs). *Geoscientific Model Development Discussions* **2023**, 1–40 (2023). ISBN: 1991-962X Publisher: Göttingen, Germany. 593  
594  
595  
596  
597  
598  
599

599 [27] Szeliski, R. in *Deep Learning* 187–271 (Springer International Publishing, Cham,  
600 2022). URL [https://link.springer.com/10.1007/978-3-030-34372-9\\_5](https://link.springer.com/10.1007/978-3-030-34372-9_5). Series Title:  
601 Texts in Computer Science.

602  
603  
604  
605  
606  
607  
608  
609  
610  
611  
612  
613  
614  
615  
616  
617  
618  
619  
620  
621  
622  
623  
624  
625  
626  
627  
628  
629  
630  
631  
632  
633  
634  
635  
636  
637  
638  
639  
640  
641  
642  
643  
644

## Appendix A List of CMIP6 models for training and testing

**Table A1** Reference CMIP6 models that are considered for the classification of SLP. The ordering follows the research group name (2nd column). The training runs are the first of available runs (in lexicographic order). The test runs are the third in lexicographic order.

Model name	Group name	Training run	Test run
BCC-CSM2-MR	BCC	r1i1p1f1	r3i1p1f1
FGOALS-g3	CAS	r1i1p1f1	r4i1p1f1
CanESM5	CCCma	r1i1p1f1	r2i1p1f1
CNRM-CM6-1	CNRM-CERFACS	r1i1p1f2	r3i1p1f2
ACCESS-ESM1-5	CSIRO	r1i1p1f1	r3i1p1f1
EC-Earth3	EC-Earth-Consortium	r1i1p1f1	r4i1p1f1
INM-CM5-0	INM	r1i1p1f1	r3i1p1f1
IPSL-CM6A-LR	IPSL	r1i1p1f1	r3i1p1f1
MIROC6	MIROC	r1i1p1f1	r3i1p1f1
HadGEM3-GC31-LL	MOHC	r1i1p1f3	r3i1p1f3
MPI-ESM1-2-LR	MPI-M	r1i1p1f1	r3i1p1f1
MRI-ESM2-0	MRI	r1i1p1f1	r2i1p1f1
CESM2	NCAR	r1i1p1f1	r3i1p1f1
NorCPM1	NCC	r1i1p1f1	r4i1p1f1
KACE-1-0-G	NIMS-KMA	r1i1p1f1	r3i1p1f1
NESM3	NUIST	r1i1p1f1	r3i1p1f1

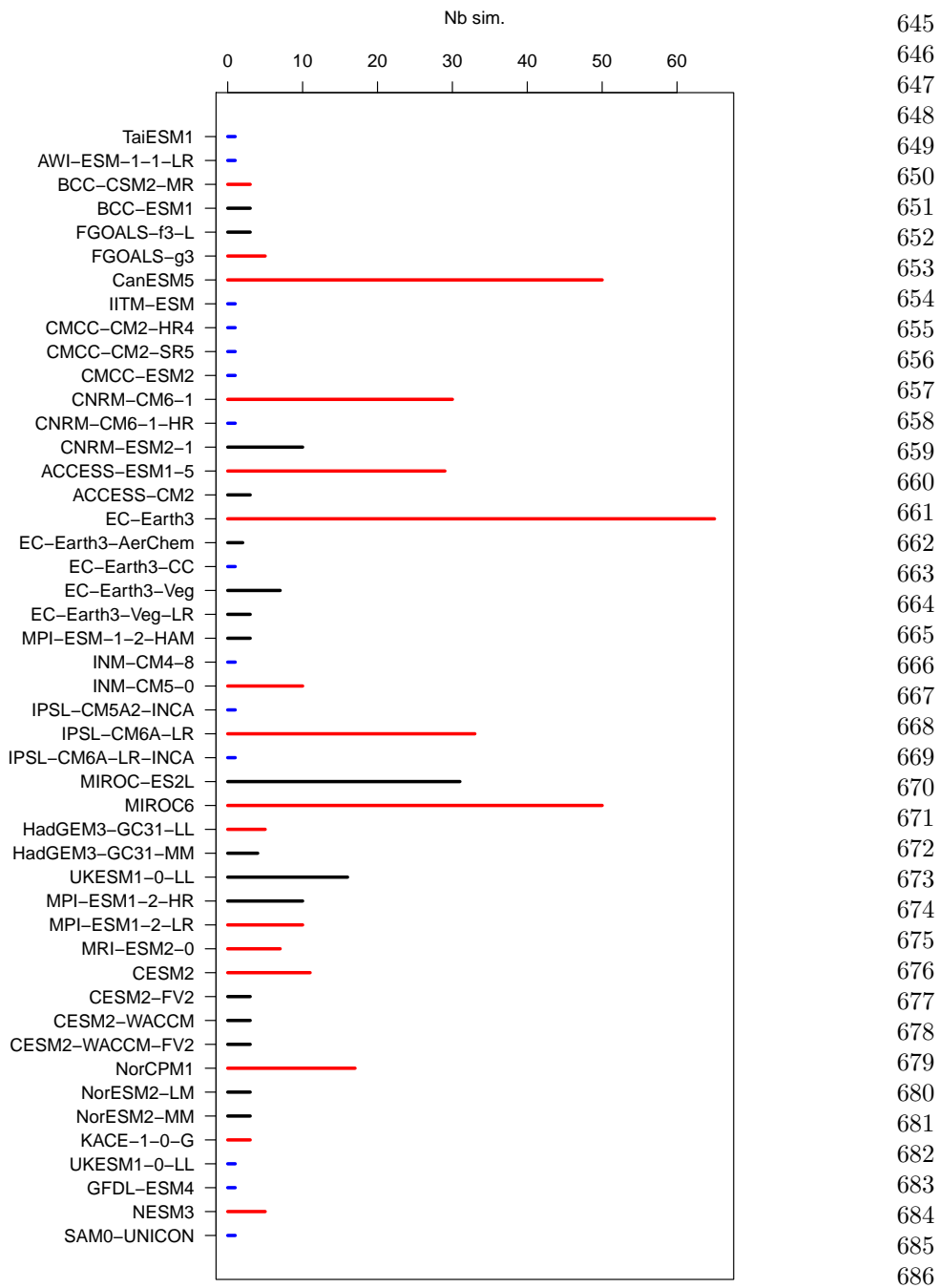


**Fig. A1** List of CMIP6 models that are available on the IPSL computing server (horizontal axis) and number of runs per model. The red lines indicate the reference models that are used in this study (in Table A1). The black lines are for models with more than 2 simulations and that are used in the "sorority" experiments. The blue lines are for models with 1 simulation and are not used in this paper. The run of UKESM1-0-LL (bottom of the figure) was run by the NIMS-KMA group (who produced the KACE-1-0-G runs).